

Lawrence Berkeley National Laboratory

Recent Work

Title

Ne-H-H POTENTIAL ENERGY SURFACE INCLUDING ELECTRON CORRELATION

Permalink

<https://escholarship.org/uc/item/6dd7p42v>

Authors

Birks, John W.
Johnston, Harold S.
Schaefer, Henry P.

Publication Date

1975-03-01

0 0 0 0 4 3 0 2 8 4 3

Submitted to Journal of Chemical Physics

LBL-3753
Preprint (.)

RECEIVED
LAWRENCE
RADIATION LABORATORY

JUN 6 1975

LIBRARY AND
DOCUMENTS SECTION

Ne-H-H POTENTIAL ENERGY SURFACE
INCLUDING ELECTRON CORRELATION

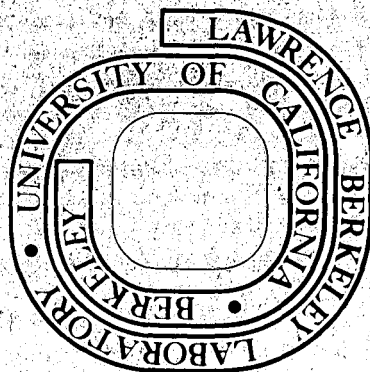
John W. Birks, Harold S. Johnston, and
Henry F. Schaefer III

March 1975

Prepared for the U. S. Energy Research and
Development Administration under Contract W-7405-ENG-48

For Reference

Not to be taken from this room



LBL-3753
(.)

DISCLAIMER

This document was prepared as an account of work sponsored by the United States Government. While this document is believed to contain correct information, neither the United States Government nor any agency thereof, nor the Regents of the University of California, nor any of their employees, makes any warranty, express or implied, or assumes any legal responsibility for the accuracy, completeness, or usefulness of any information, apparatus, product, or process disclosed, or represents that its use would not infringe privately owned rights. Reference herein to any specific commercial product, process, or service by its trade name, trademark, manufacturer, or otherwise, does not necessarily constitute or imply its endorsement, recommendation, or favoring by the United States Government or any agency thereof, or the Regents of the University of California. The views and opinions of authors expressed herein do not necessarily state or reflect those of the United States Government or any agency thereof or the Regents of the University of California.

-iii-

Ne-H-H Potential Energy Surface
Including Electron Correlation

by

John W. Birks*, Harold S. Johnston

and

Henry F. Schaefer III

Department of Chemistry and
Inorganic Materials Research Division
Lawrence Berkeley Laboratory
University of California
Berkeley, California 94720

*Present Address:

Department of Chemistry
University of Illinois at Urbana-Champaign
Urbana, Illinois 61801

ABSTRACT

An ab initio calculation of the Ne-H-H potential energy hypersurface for a wide range of H₂ internuclear separation ($0.8 \leq R \leq 5.0$ Bohr) and Ne-H₂ separation ($2.5 \leq X \leq 6.0$ Bohr) is reported. Calculations were carried out for both the collinear and perpendicular bisector geometries.

For the perpendicular bisector geometry, the potential surface has the property previously found for He-H₂ of exerting a contractive force on the H₂ molecule as the noble gas atom approaches. The surface demonstrates a cross-over point near 3.0 Bohr where the contractive force changes to a stretching force.

Analytic fits to the potential energy surface are presented and discussed in detail. In particular, the "dumbbell" model was not found to provide a good description of the potential surface. Because of the wide range in values of X and R for which points were calculated, the surface reported here should be useful for trajectory studies of diatomic dissociation and atom recombination.

I. Introduction

The present paper represents one step in a theoretical study of the bimolecular dissociation of diatomic molecules. Accordingly we have carried out an ab initio calculation of the Ne-H-H potential energy surface. Previous studies by other investigators of the He-H₂ interaction potential have been reported for relatively large separations between the He atom and H₂ molecule and for small changes in the H₂ internuclear distance.¹⁻⁴ Thus, the He-H₂ surface has not been defined in the region where bimolecular dissociation and three body atom recombination occur. We have studied the Ne-H-H surface over a large range of atom-molecule separations ($2.5 \leq X \leq 6.0$ Bohr) and internuclear distances ($0.8 \leq R \leq 5.0$ Bohr). Figure 1 is the coordinate system for representing the potential energy surface. Calculations were made for the two symmetrical arrangements of atoms, $\theta = 0^\circ$ and 90° . We present analytic fits to the Ne-H-H collinear surface and to the entire Ne-H-H hypersurface assuming an angular form similar to that found for He-H₂.

II. Theoretical Approach

For neon the (9s5p) Gaussian basis of Van Duijneveldt⁵ contracted to (5s3p) was used. The exponents and contraction coefficients for this (9s5p/5s3p) basis set are provided in Table I.

TABLE I. NEON (9s5p/5s3p) BASIS SET

Basis Function	Gaussian Exponent	Contraction Coefficient	Symmetry
1	16501.214801	.000815	1s
1	2477.76179	.006260	1s
1	566.109589	.031596	1s
1	161.628536	.116378	1s
1	53.29324	.301929	1s
2	19.488234		1s
3	7.60176		1s
4	1.632772		1s
5	.481315		1s
6	55.030482	.016995	2p _x
6	12.501192	.106925	2p _x
6	3.69786	.320808	2p _x
7	1.147741		2p _x
8	.331057		2p _x
9	55.030482	.016995	2p _y
9	12.501192	.106925	2p _y
9	3.69786	.320808	2p _y
10	1.147741		2p _y
11	.331057		2p _y
12	55.030482	.016995	2p _x

TABLE I. (Continued)

Basis Function	Gaussian Exponent	Contraction Coefficient	Symmetry
12	12.501192	.106925	2p _z
12	3.69786	.320808	2p _z
13	1.147741		2p _z
14	.331057		2p _z

The hydrogen basis set was determined by contracting the (5slp) basis set of Huzinaga⁶ to (3slp) followed by optimization of the s and p Gaussian exponent scale factors by finding the lowest full CI energy for the H₂ molecule. For an s scale factor of 1.20 and p scale factor of 0.85 the dissociation energy was found to be 0.168399 Hartree or 105.7 kcal/mole. The resulting hydrogen basis set is given in Table II. A total of 26 basis functions were used; 14 functions centered on neon, and 6 functions centered on each of the hydrogen atoms.

Calculations were made for the collinear (C_{∞v} symmetry) and perpendicular bisector (C_{2v} symmetry) geometries. In the C_{2v} case 13 orbitals transform as a₁ symmetry, 1 as a₂ symmetry, 4 as b₁ symmetry, 8 as b₂ symmetry; and the core may be written 1a₁² 2a₁² 3a₁² 1b₁² 1b₂². For the 2-configuration MCSCF calculation the two configurations that were considered are core-4a₁² and core-2b₂².

In the collinear case there are 16 orbitals of σ symmetry, 5 orbitals of π_x symmetry, 5 orbitals of π_y symmetry, and the core is 1σ² 2σ² 3σ² 1π_x² 1π_y². The two configurations used in the MCSCF calculations are core-4σ² and core-5σ². In addition to the MCSCF calculation, a full 2-electron CI calculation (for a total of 111 configurations) was carried out using the orbitals from the collinear MCSCF wave functions. This type of CI provides a nearly quantitative picture of the dissociation of H₂ in the presence of a Ne atom described at the Hartree-Föch level.

III. Results

The results of the Ne-H-H potential energy surface calculations are summarized in Table III. The coordinate system for representing

TABLE II. HYDROGEN BASIS SET

Basis Function	Gaussian Exponent	Contraction Coefficient	Symmetry
1	48.44160	.025374	1s
1	7.28352	.189684	1s
1	1.65168	.852933	1s
2	.46238		1s
3	.14587		1s
4	.7225		2p _x
5	.7225		2p _y
6	.7225		2p _z

TABLE III. RESULTS OF POTENTIAL ENERGY SURFACE CALCULATIONS, ATOMIC UNITS

θ	R	X	V_{MCSCF}	V'_{MCSCF}	V_{CI}	V'_{CI}	$V'_{CI} - V'_{MCSCF}$	%
0	0.8	2.5	-129.36975	.14734	-129.39333	.14592	-.00142	0.97
0	0.8	3.0	-129.46265	.05586	-129.48623	.05302	-.00284	5.36
0	0.8	3.5	-129.49721	.01988	-129.52072	.01853	-.00135	7.29
0	0.8	4.0	-129.50971	.00738	-129.53313	.00612	-.00126	20.58
0	0.8	6.0	-129.51722	-.00013	-129.53938	-.00013	.00000	0.00
0	1.1	2.5	-129.47985	.17074	-129.50334	.16713	-.00361	2.16
0	1.1	3.0	-129.58100	.06959	-129.60610	.06437	-.00522	8.11
0	1.1	3.5	-129.62684	.02375	-129.64672	.02375	.00000	0.00
0	1.1	4.0	-129.64228	.00831	-129.66212	.00835	.00004	0.48
0	1.1	6.0	-129.65068	-.00009	-129.67056	-.00009	.00000	0.00
0	1.4	2.5	-129.48243	.19580	-129.50552	.19015	-.00585	3.08
0	1.4	3.0	-129.59194	.08629	-129.61831	.07736	-.00893	11.54
0	1.4	3.5	-129.64782	.03039	-129.66544	.03021	-.00018	0.60
0	1.4	4.0	-129.66695	.01126	-129.68441	.01124	-.00002	0.18
0	1.4	6.0	-129.67825	-.00004	-129.69569	-.00004	.00000	0.00

00004302848

TABLE III. (Continued)

Θ	R	X	V_{MCSCF}	V'_{MCSCF}	V_{CI}	V'_{CI}	$V'_{CI} - V'_{MCSCF}$	%
0	1.7	2.5	-129.44416	.22483	-129.46612	.21773	-.00710	3.26
0	1.7	3.0	-129.56456	.10443	-129.59164	.09221	-.01222	13.25
0	1.7	3.5	-129.61558	.05341	-129.64554	.03831	-.01510	39.41
0	1.7	4.0	-129.63765	.03134	-129.66876	.01509	-.01625	107.69
0	1.7	6.0	-129.66893	.00006	-129.68379	.00006	.00000	0.00
0	2.0	2.5	-129.38223	.26492	-129.40305	.25629	-.00863	3.36
0	2.0	3.0	-129.52276	.12439	-129.54993	.10941	-.01498	13.69
0	2.0	3.5	-129.57907	.06808	-129.61132	.04802	-.02006	41.77
0	2.0	4.0	-129.60482	.04233	-129.63940	.01994	-.02239	112.28
0	2.0	6.0	-129.64696	.00019	-129.65915	.00019	.00000	0.00
0	3.0	3.0	-129.34044	.23346	-129.36475	.21363	-.01983	9.28
0	3.0	3.5	-129.44020	.13370	-129.47745	.10093	-.03277	32.46
0	3.0	4.0	-129.47829	.09561	-129.52918	.04920	-.04641	94.32
0	3.0	4.5	-129.55172	.02218	-129.55648	.02190	-.00028	1.27
0	3.0	5.0	-129.56471	.00919	-129.56928	.00910	-.00009	0.98
0	3.0	6.0	-129.57262	.00128	-129.57711	.00127	-.00001	0.78

TABLE III. (Continued)

θ	R	X	V_{MCSCF}	V'_{MCSCF}	V_{CI}	V'_{CI}	$V'_{CI} - V'_{MCSCF}$	%
0	4.0	3.5	-129.28293	.25573	-129.31402	.22553	-.03020	13.39
0	4.0	4.0	-129.36637	.17229	-129.42273	.11682	-.05547	47.48
0	4.0	4.5	-129.48125	.05741	-129.48258	.05697	-.00044	0.77
0	4.0	5.0	-129.51286	.02580	-129.51388	.02567	-.00013	0.50
0	4.0	5.5	-129.52775	.01091	-129.52868	.01087	-.00004	0.36
0	4.0	6.0	-129.53429	.00437	-129.53520	.00435	-.00002	0.45
0	5.0	4.0	-129.23230	.29621	-129.27227	.25638	-.03983	15.53
0	5.0	4.5	-129.39726	.13125	-129.39797	.13068	-.00057	0.43
0	5.0	5.0	-129.46602	.06249	-129.46626	.06239	-.00010	0.16
0	5.0	5.5	-129.50067	.02784	-129.50084	.02781	-.00003	0.10
0	5.0	6.0	-129.51671	.01180	-129.51686	.01179	-.00001	0.08

00004302849

TABLE III. (Continued)

Θ	R	X	V_{MCSCF}	V'_{MCSCF}
90	0.8	3.0	-129.47120	.04589
90	0.8	3.5	-129.50606	.01103
90	0.8	4.0	-129.51363	.00346
90	1.1	3.0	-129.60615	.04444
90	1.1	3.5	-129.63863	.01196
90	1.1	4.0	-129.64660	.00399
90	1.4	2.5	-129.37819	.30001
90	1.4	3.0	-129.64076	.03744
90	1.4	3.5	-129.66570	.01250
90	1.4	4.0	-129.67366	.00454
90	1.7	2.5	-129.52825	.14074
90	1.7	3.0	-129.63324	.03575
90	1.7	3.5	-129.65558	.01341
90	1.7	4.0	-129.66377	.00522

TABLE III. (Continued)

θ	R	X	V_{MCSCF}	V'_{MCSCF}
90	2.0	2.5	-129.53945	.10770
90	2.0	3.0	-129.61177	.03538
90	2.0	3.5	-129.63276	.01439
90	2.0	4.0	-129.64127	.00588
90	3.0	2.5	-129.50580	.06810
90	3.0	3.5	-129.55928	.01462
90	3.0	4.0	-129.56744	.00646

points on the surface was previously presented as Figure 2. The two values of θ for which points were calculated are 0° and 90° for the collinear and perpendicular bisector geometries respectively.

For each value of the hydrogen internuclear separation R , a calculation was made with the Ne atom held at an essentially infinite distance, $X = 100$ Bohr. This facilitated the separation of the Ne-H-H potential energy into two parts, the H_2 potential energy and the Ne- H_2 potential energy of interaction. The H_2 potential energy is well known, both from theoretical calculations and spectroscopic studies. Of interest here is the Ne- H_2 interaction energy V' , defined by

$$V'(X,R,\theta) = V(X,R,\theta) - V(\infty,R,\theta) \quad (1)$$

The values of V'_{MCSCF} and V'_{CI} are provided in Table III. Also provided are the differences, $V'_{CI} - V'_{MCSCF}$, and percent differences.

IV. Fit of the Ne- H_2 Potential Energy of Interaction to an Analytic Form

Figure 2 presents plots of $\ln V'_{CI}(X,R,0^\circ)$ against R for the various values of X . The linearity in these plots indicates that for the collinear geometry the potential energy of interaction $V'(X,R,0^\circ)$ may be represented by a function of the form

$$V'(X,R,0^\circ) = A'(X) \exp[\alpha(X) R] \quad (2)$$

where $\alpha(X)$ is the slope of the line and $A'(X)$ is the intercept. The slopes and intercepts were determined from least squares fits to the calculated points for $X = 2.5, 3.0, 3.5$ and 4.0 . A fit of $\alpha(X)$ to a second order polynomial in X of the form

$$\alpha(X) = a + bX + cX^2 \quad (3)$$

yielded the results $a = -0.74079$, $b = 0.60491$ and $c = -0.04930$. The fit of this function to the four values of $\alpha(X)$ is shown in Fig. 3. For the intercepts, a plot of $\ln A(X)$ against X (Fig. 4) gave a linear plot with slope -2.2909 and intercept 3.4267 . The linearity of this plot is to be expected since in the limit as R goes to zero the H_2 molecule becomes a He atom, and the interaction between the He and Ne atoms would be expected to be purely repulsive, varying as $e^{-\beta X}$. Combining these results, we have for the Ne- H_2 potential energy of interaction for the collinear geometry

$$V'(X, R, 0^0) = \exp[A + BX + CR + DXR + EX^2R] \quad (4)$$

where

$$A = 3.4267, B = -2.2909, C = -0.74079, D = 0.60491, E = -0.04930 \quad (5)$$

The variance of the fit can be lowered somewhat by considering the simultaneous variation of all five parameters. A general least squares fitting program was used to find a new set of parameters,

resulting in a reduction of the variance by about a factor of three. The "initial guess" for this calculation was the set of parameters (5). The new parameters thus obtained are

$$\begin{aligned} A = 3.0450, B = -2.1583, C = -0.46568, D = \\ 0.47356, E = -0.03633 \end{aligned} \quad (6)$$

The possibility of obtaining an even better fit by including the term FXR^2 inside the exponential function of (4) was also investigated. The parameters obtained for this six parameter fit are given by (7).

$$\begin{aligned} A = 3.4424, B = -2.3223, C = -0.73964, D = \\ 0.62100, E = -0.04568, F = -0.005782 \end{aligned} \quad (7)$$

This resulted in the best fit to the calculated points on the collinear potential energy surface.

An optimized set of parameters was also obtained for the so-called "dumbbell potential". This is the empirical form that has often been used in vibrational energy transfer theory,⁷ and has been used in Keck's phase space theory of dissociation and atom recombination.⁸ For this model of the interaction potential one assumes that there is a repulsive term of the form $Ae^{-\beta r}$ between the inert gas atom and each of the two atoms of the diatomic molecule. Here r is simply the distance between the inert gas atom Ne and the atom of interest. For a homonuclear diatomic molecule, β is the same for each atom so that the total interaction potential may be written

$$V' = Ae^{-\beta r_A} + Ae^{-\beta r_B} \quad (8)$$

where the A and B subscripts on r refer to the two different hydrogen atoms. For the collinear case we may replace r_A and r_B by $X - \frac{1}{2} R$ and $X + \frac{1}{2} R$, respectively. We then have for the interaction potential the expression

$$V' = Ae^{-\beta X} [e^{1/2 \beta R} + e^{-1/2 \beta R}] \quad (9)$$

The least squares parameters obtained for a fit to this form of the interaction potential are

$$A = 2.2828, \beta = 1.500 \quad (10)$$

This form of the interaction potential is desirable since only two fitting parameters are required, and because Equation (8) applies to all possible arrangements of the atoms rather than only the collinear arrangement. The variance for the fit was about an order of magnitude larger than that of those fits previously described, however.

The dumbbell potential was also found to be inadequate for the He-H₂ interaction potential by Gordon and Secrest.³ Dimpfl⁹ has suggested that this form for the interaction potential might be improved upon by including an attractive term centered at the diatomic molecule center of mass. For the collinear case the improved dumbbell interaction potential suggested by Dimpfl has

the form

$$V' = Ae^{-\beta X} [e^{-\beta R/2} + e^{\beta R/2}] + Be^{-\gamma X} \quad (11)$$

The least squares parameters obtained for this four parameter fit are

$$A = 1.5972, \beta = 1.183, B = -0.11137, \gamma = 0.3235 \quad (12)$$

Increasing the number of parameters from two to four did not substantially improve the dumbbell form of the interaction potential, however. In Table IV a comparison is made between the actual points on the collinear surface and those calculated from each of the analytic fits described. The variance for each fit is also given in Table IV.

For three-dimensional trajectory calculations it is necessary to have an analytic form of the potential energy for all possible arrangements of the atoms. Thus in the present case it is necessary to be able to represent the potential energy for the collinear geometry, the perpendicular bisector geometry, and all angles in between. Since no calculations were made at angles other than 0° and 90° it was necessary to rely on the previous work of Roberts,¹ Krauss and Mies² and Gordon and Secrest³ for the He-H₂ potential energy to arrive at a reasonable way of representing the angular part of the potential energy surface. Accordingly, the interaction potential was assumed to be separable into two parts,

$$V'(X,R,\theta) = V_1'(X,R) V_2'(R,\theta) \quad (13)$$

Table IV. Analytic Fits to the Collinear Surface*

X	R	V_{CI}^1	Fit 44	Fit 45	Fit 46	Fit 49	Fit 51
2.5	0.8	145.92	145.17	141.85	142.17	127.35	135.19
3.0	0.8	53.02	52.77	53.79	51.52	60.16	60.08
3.5	0.8	18.53	18.81	20.10	18.33	28.42	20.71
4.0	0.8	6.12	6.57	7.40	6.40	13.43	0.79
2.5	1.1	167.13	166.82	164.37	165.17	146.11	152.64
3.0	1.1	64.37	63.75	64.94	63.16	69.02	69.74
3.5	1.1	27.75	23.71	25.15	23.55	32.61	26.05
4.0	1.1	8.35	8.58	9.55	8.57	15.40	3.75
2.5	1.4	190.15	191.70	190.46	191.40	172.28	176.48
3.0	1.4	77.36	77.02	78.40	77.20	81.39	82.93
3.5	1.4	30.23	29.90	31.47	30.16	30.21	33.36
4.0	1.4	11.24	11.21	12.31	11.41	18.16	7.79
2.5	1.7	217.73	220.28	220.69	221.22	207.21	207.46
3.0	1.7	92.21	93.05	94.66	94.06	97.89	100.08
3.5	1.7	38.31	37.69	39.37	38.47	46.25	42.85
4.0	1.7	15.09	14.64	15.87	15.14	21.85	13.04
2.5	2.0	256.29	253.14	255.73	255.01	252.68	246.56
3.0	2.0	109.41	112.42	114.28	114.25	119.37	121.71
3.5	2.0	48.02	47.52	49.25	48.90	56.39	54.82
4.0	2.0	19.94	19.12	20.47	20.00	26.64	19.67
3.0	3.0	213.63	211.13	214.14	213.55	243.36	236.35
3.5	3.0	100.93	102.90	103.91	105.94	114.97	118.26

Table IV. (cont'd.)

X	R	V_{CI}^1	Fit 44	Fit 45	Fit 46	Fit 49	Fit 51
4.0	3.0	49.20	46.57	47.75	49.07	54.31	54.78
4.5	3.0	21.90	19.58	20.78	21.23	25.66	21.25
5.0	3.0	9.10	7.64	8.56	8.57	12.12	4.04
3.5	4.0	225.53	222.78	219.25	220.41	241.29	237.25
4.0	4.0	116.82	113.42	111.41	115.00	113.99	120.64
4.5	4.0	56.97	52.32	52.64	54.76	53.85	57.69
5.0	4.0	25.67	21.87	23.13	23.80	25.44	24.21
5.5	4.0	10.87	8.28	9.45	9.44	12.02	6.83
4.0	5.0	256.38	276.19	259.92	257.31	240.82	240.96
4.5	5.0	130.68	139.81	133.35	134.12	113.77	124.28
5.0	5.0	62.39	62.57	62.48	62.36	53.75	61.06
5.5	5.0	27.81	24.75	26.73	25.87	25.39	27.23
6.0	5.0	11.79	8.66	10.44	9.57	12.00	9.48
Variance			6.14×10^{-4}	2.10×10^{-4}	1.51×10^{-4}	4.08×10^{-3}	2.64×10^{-3}

*Energies are in millihartrees, distances in Bohr.

one part depending only on the variables X and R and one part depending only on the variables R and θ . The latter part, $V_2'(R, \theta)$, was represented by the following function.

$$V_2'(R, \theta) = 1 + \gamma P_2(\cos \theta) + \delta P_2(\cos \theta) R \quad (14)$$

Here, P_2 is a Legendre polynomial so that

$$P_2(\cos \theta) = \frac{3}{2} \cos^2 \theta - \frac{1}{2} \quad (15)$$

The coefficients γ and δ were determined by considering the ratio of the potential energy of interaction for the perpendicular bisector geometry $V'(X, R, 90^\circ)$ to that for the collinear geometry $V'(X, R, 0^\circ)$, which is given by

$$\frac{V'(X, R, 90^\circ)}{V'(X, R, 0^\circ)} = \frac{1 - 1/2\gamma - 1/2 \delta R}{1 + \gamma + \delta R} \quad (16)$$

The following values for γ and δ fit this ratio exactly for $X = 4.0$ and the two extreme values of $R = 0.8$ and $R = 3.0$.

$$\gamma = 0.05623 \text{ and } \delta = 0.4399 \quad (17)$$

It was necessary, unfortunately, to use the MCSCF results for $V'(X, R, 90^\circ)$. In the limit of no "correlation energy of interaction" (X large; R small for $\theta = 0^\circ$, R large for $\theta = 90^\circ$) the MCSCF and CI results for the interaction energy must be identical. It can be seen in Table III that this is certainly the case for the collinear geometry; the values of V'_{CI} and V'_{MCSCF} being nearly the same except when the Ne atom is very near one of the hydrogen

atoms (X small, R large). For this reason the coefficients γ and δ were determined at the largest value of X for which there was still a sufficient interaction, so that $V'_{CI}(X,R,0^\circ)$ and $V'_{MCSCF}(X,R,90^\circ)$ contained a minimum amount of correlation energy. The ratio of interaction energies, Equation (16), does not vary with changes in X. Table V compares all such ratios with those calculated from this equation. The ratios listed in Table V are not all constant over changes in X. However, the variation that is present is consistent with the fact that V'_{MCSCF} does not include as much of the correlation energy at small values of X as does V'_{CI} .

For the calculation of 3-D trajectories, to be described in a subsequent article, the form of the interaction potential used is

$$V'(X,R,\theta) = \frac{1 + \gamma P_2(\cos\theta) + \delta P_2(\cos\theta) R}{1 + \gamma + \delta R} V'(X,R,0^\circ) \quad (18)$$

where $V'(X,R,0^\circ)$ is given by Equation (4). For the potential energy of the hydrogen molecule a Morse potential is used. The total potential energy hypersurface is then given by

$$V(X,R,\theta) = D_e [1 - \exp(-1.0274r)]^2 + V'(X,R,\theta) \quad (19)$$

where D_e is the dissociation energy, and

$$r = R - R_e \quad (20)$$

where R_e is the equilibrium internuclear distance, 1.40 Bohr.

Table V. Values of $\frac{V'(X,R,90^\circ)}{V'(X,R,0^\circ)}$

X \ R	0.8	1.1	1.4	1.7	2.0	3.0
3.0	0.866	0.690	0.484	0.388	0.323	
3.5	0.595	0.504	0.414	0.350	0.300	0.145
4.0	0.565	0.478	0.404	0.346	0.295	0.131
Fit to Eq. 55	0.565	0.474	0.397	0.331	0.275	0.131

V. Discussion

The interesting aspect of the Gordon-Secrest³ interaction potential for He-H₂ is that as the He atom approaches the H₂ molecule for the perpendicular bisector geometry, a contractive force is exerted on the H₂ molecule. This is, of course, just the opposite effect from that predicted by the dumbbell potential, in which the force is always in the direction of stretching the H₂ internuclear distance. This effect is also present in the Krauss-Mies² He-H₂ potential. Neither Krauss and Mies nor Gordon and Secrest calculated points at sufficiently small values of X (close-in) to show that this effect is actually reversed at small values of X . Realizing that there must be some cross-over point, however, both groups of investigators required that the analytic fit be such that there is a cross-over point where the force exerted on the H₂ bond is zero. For the Gordon-Secrest fit this cross-over occurs at $X = 2.01$ Bohr, and for the Krauss-Mies fit the value is $X = 1.85$ Bohr.

In a recent article, Alexander and Berard¹⁰ presented four new ways of fitting the Gordon-Secrest points on the He-H₂ surface. They also calculated probabilities of He-H₂ vibrational energy transfer for each of their four analytic fits and for the Gordon-Secrest fit. They found that the matrix element for the $0 \rightarrow 1$ transition goes to zero for the Gordon-Secrest fit near $X = 2$. Since none of the four fits of Alexander and Berard exhibited this

feature, the transition probability changing smoothly with X , they suggested that the Gordon-Secret fit was anomalous. All four of the Alexander and Berard fits have the property that as the distance X increases the contractive force increases, with no cross-over point. This is unrealistic. As pointed out by Secret,¹¹ one would expect a cross-over point where the probability of vibrational energy transfer is reduced to zero, since at this point no force is exerted along the H_2 bond.

That such a cross-over does exist is demonstrated by the data presented in Table III for the Ne- H_2 interaction potential. Consider first the results for $X = 4.0$. In Table III it can be seen that

$$V'(R = .8) < V'(R = 1.1) < V'(R = 1.7) < V'(R = 2.0) < V'(R = 3.0) \quad (21)$$

so that the force is in the direction of contracting the H_2 internuclear distance, R . For $X = 3.5$, Eq. (21) still applies. For $X = 3.0$, however, we have

$$V'(R = .8) > V'(R = 1.1) > V'(R = 1.7) > V'(R = 2.0) > V'(R = 3.0) \quad (22)$$

and this is seen to be true for $X = 2.5$ as well. Thus, there is a cross-over point between $X = 3.0$ and $X = 3.5$. For X larger than the value of the cross-over point there is a contractive force, and for X smaller than the value of the cross-over point, there is a stretching force.

For an analytic fit, the value of X at the cross-over point may be found by taking the derivative of the interaction potential with respect to R , setting the result equal to zero, and solving for X with $R = 1.4$. The cross-over occurs at slightly different positions for different values of R . The analytic fit (Equation 18) suggested in the previous section has a cross-over at $X = 2.9$ Bohr. In consideration of this type of behavior for the interaction potential, it is not surprising that the dumbbell form for the potential results in a poor fit.

Acknowledgments

Assistance with the electronic structure calculations by Dean Liskow is gratefully acknowledged. A helpful discussion of this work with Don Secrest is also appreciated. This work was carried out under the auspices of the U.S. Energy Research and Development Administration.

REFERENCES

1. C. S. Roberts, Phys. Rev. 131, 203 (1963).
2. M. Krauss and F. H. Mies, J. Chem. Phys. 42, 2703 (1965).
3. M. D. Gordon and D. Secrest, J. Chem. Phys. 52, 120 (1970).
4. B. Tsapline and W. Kutzelnigg, Chem. Phys. Lett. 23, 173 (1973).
5. F. B. Van Duijneveltdt, RJ945, December 1971 (IBM Research Laboratory, San Jose, California 95193).
6. S. Huzinaga, J. Chem. Phys. 42, 1293 (1965).
7. J. D. Kelley and M. Wolfsberg, J. Chem. Phys. 44, 324 (1966).
D. Rapp and T. Kassal, Chem. Rev. 69, 61 (1969).
8. J. C. Keck, Adv. Atom. Mol. Phys. 8, 39 (1972).
9. W. L. Dimpfl, Ph.D. Thesis, University of California, Berkeley (August 1973). Available as report LBL-1873.
10. M. H. Alexander and E. V. Bernard, J. Chem. Phys. 60, 3950 (1974).
11. D. Secrest, J. Chem. Phys. 61, 3867 (1974).

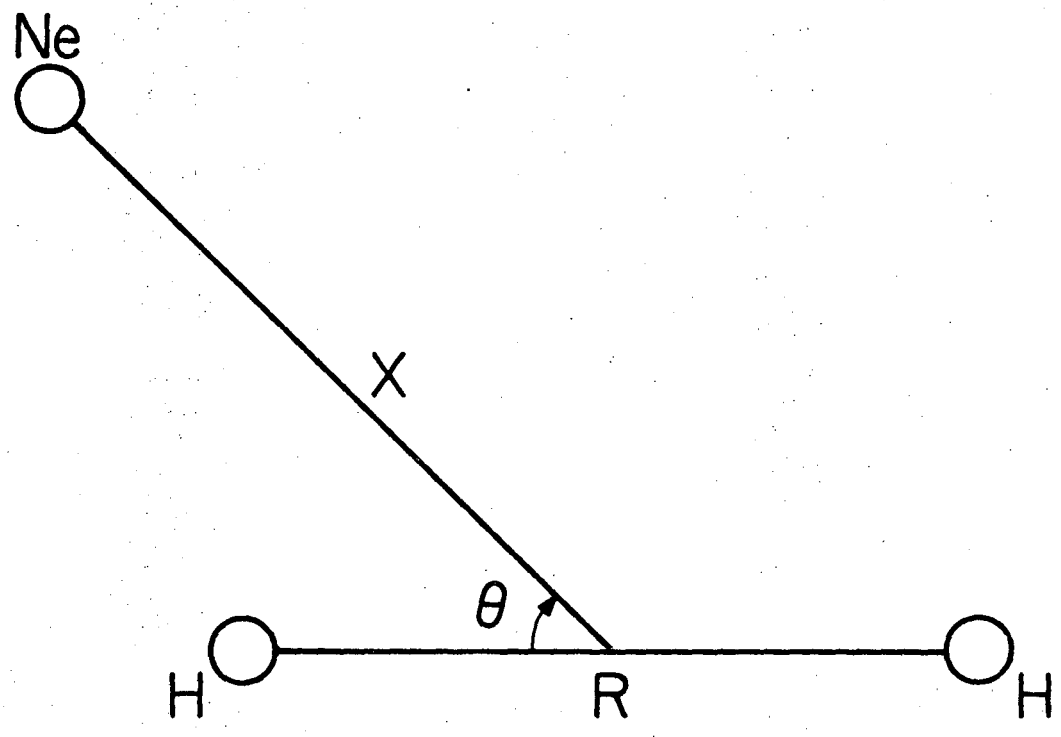
TITLES TO FIGURES

Figure 1 - Coordinate system for representing the Ne-H-H potential energy surface.

Figure 2 - Plots of $V'(X,R)$ vs. R for fixed values of X and $\theta = 0^\circ$. The linearity of these plots suggests one way of fitting the collinear surface.

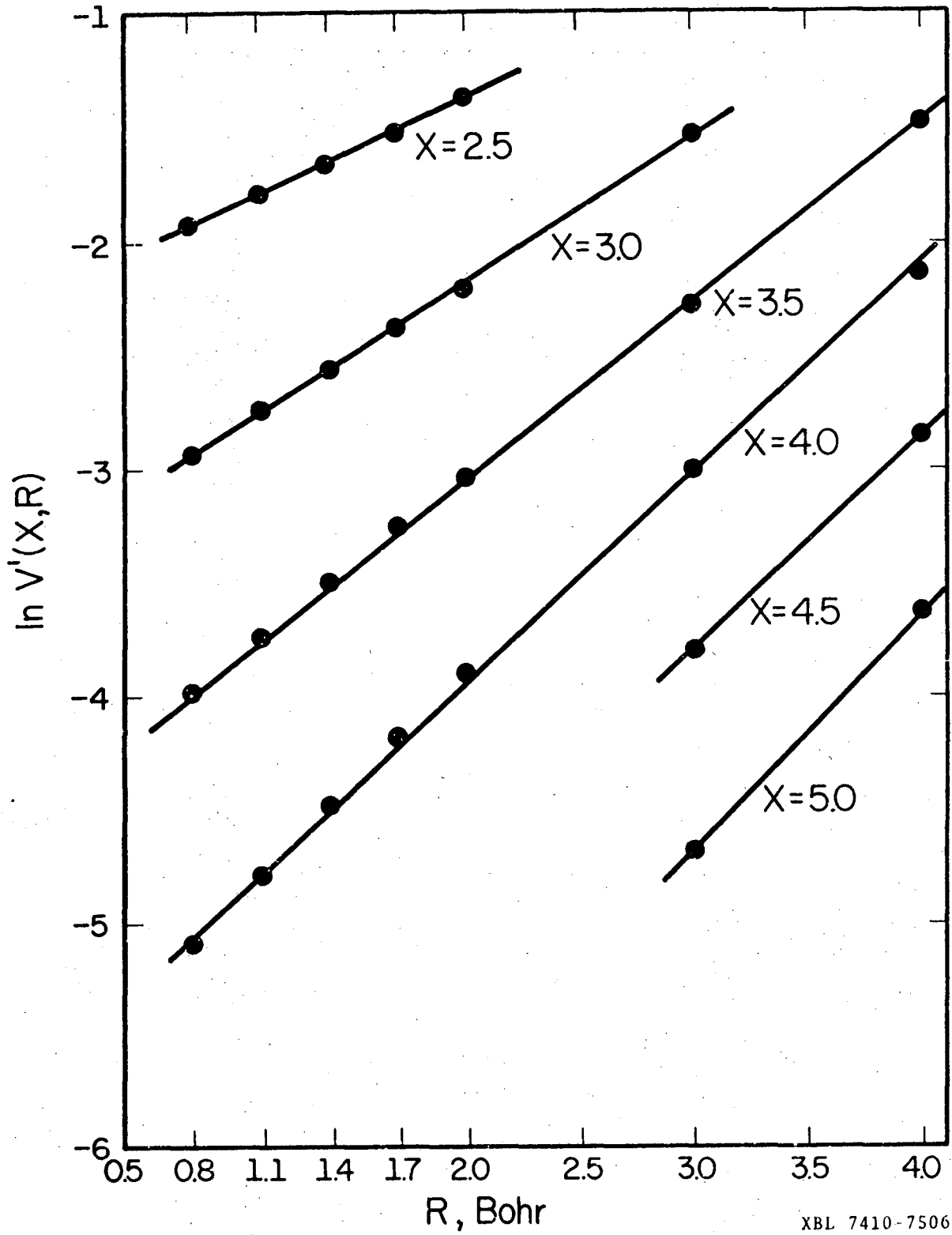
Figure 3 - Comparison of $\alpha(X)$ of equation 42 with the slopes of the lines of Fig. 3 for $X = 2.5, 3.0, 3.5,$ and 4.0 .

Figure 4 - Plot of the \log_e of the intercept, A' , of Fig. 3 versus X .



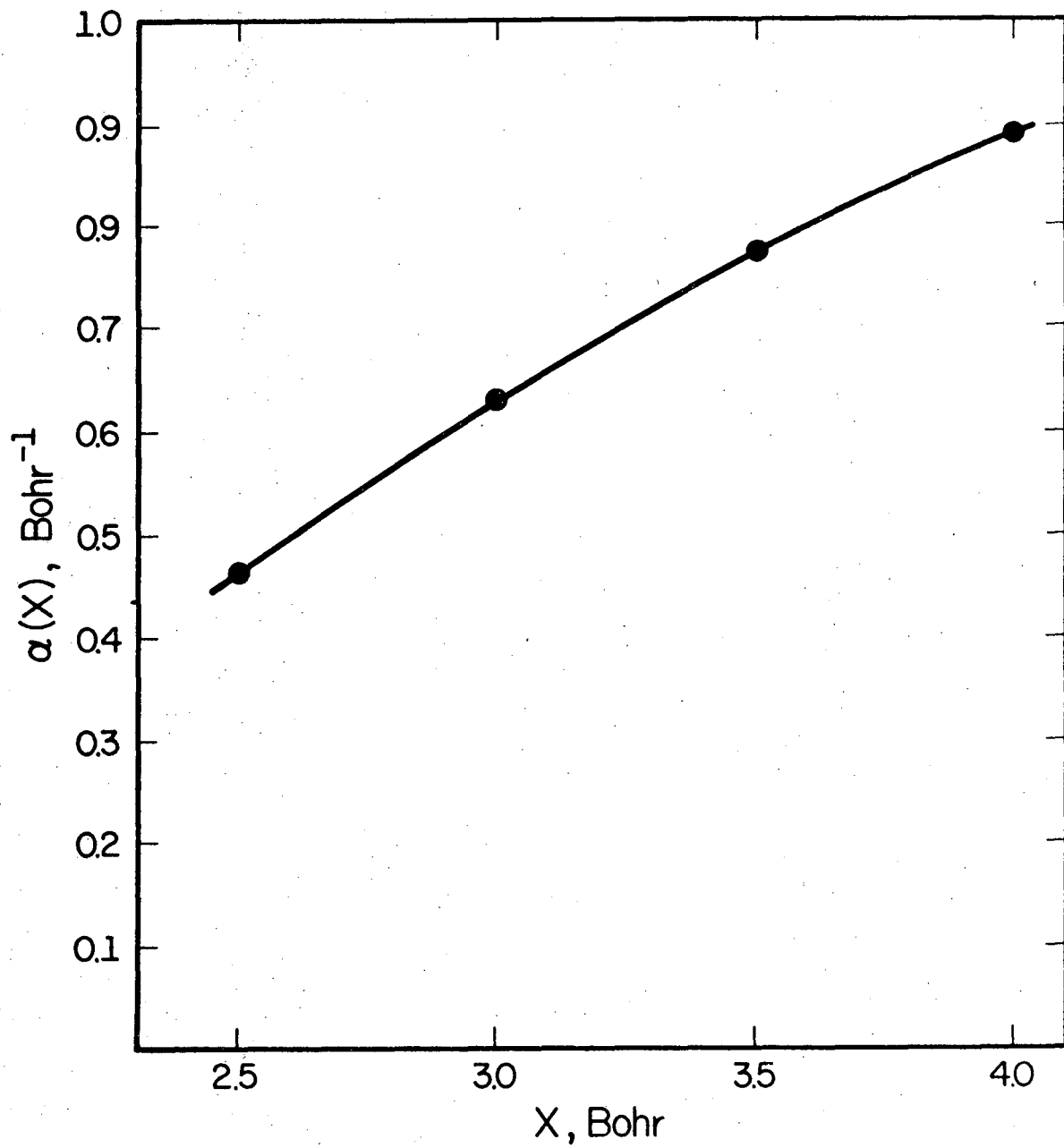
XBL 7410-7505

Fig. 1



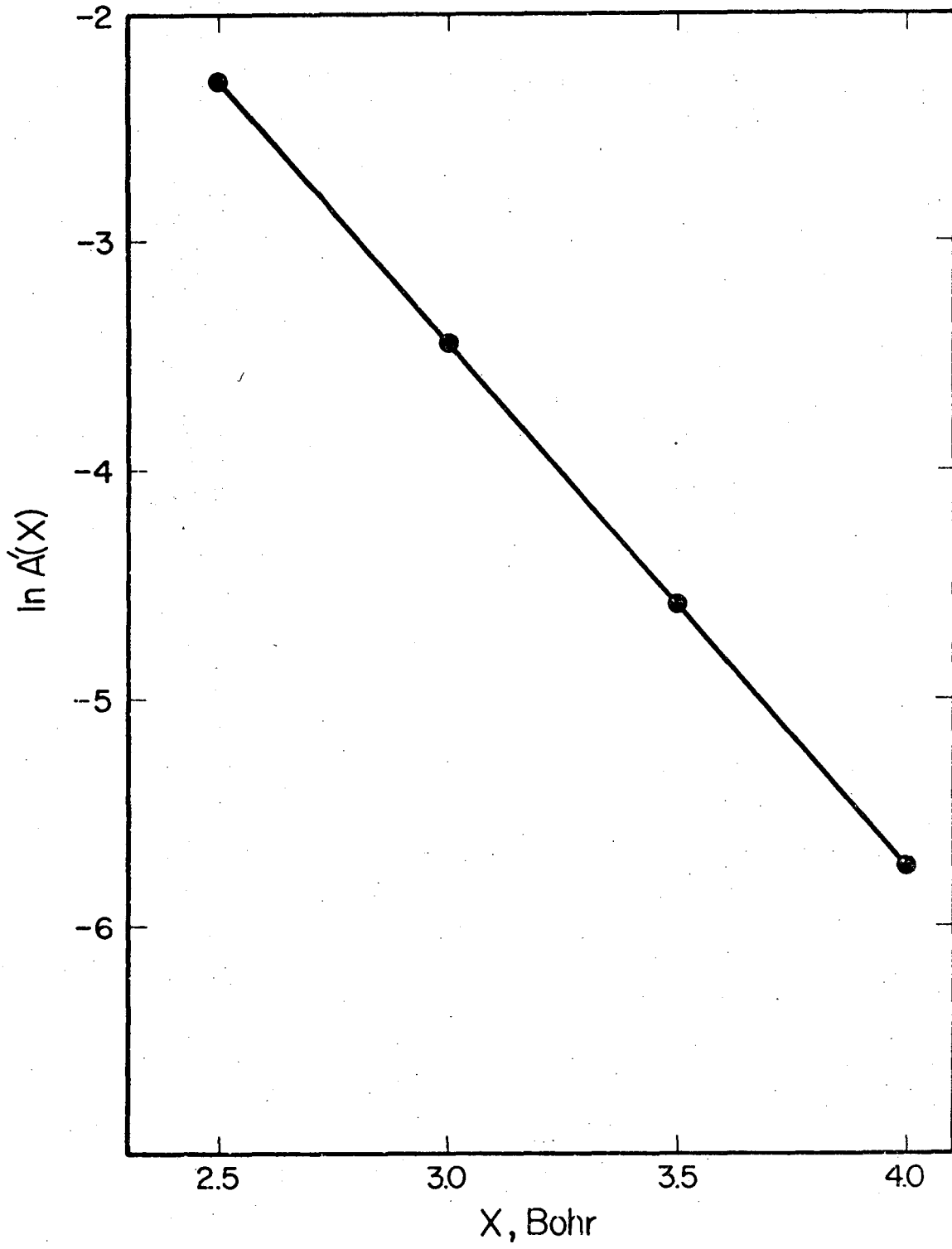
XBL 7410-7506

Fig. 2



XBL 7410-7507

Fig. 3



XEL 7410-7508

Fig. 4

LEGAL NOTICE

This report was prepared as an account of work sponsored by the United States Government. Neither the United States nor the United States Energy Research and Development Administration, nor any of their employees, nor any of their contractors, subcontractors, or their employees, makes any warranty, express or implied, or assumes any legal liability or responsibility for the accuracy, completeness or usefulness of any information, apparatus, product or process disclosed, or represents that its use would not infringe privately owned rights.

TECHNICAL INFORMATION DIVISION
LAWRENCE BERKELEY LABORATORY
UNIVERSITY OF CALIFORNIA
BERKELEY, CALIFORNIA 94720